actuators

MDPI

Article

A Biomimetic Soft Robot for In-Pipe Inspection: Design, Development, and Experimental Validation

Leonarda Došen, Jan Pelić, Goran Gregov and Ervin Kamenar *

University of Rijeka, Faculty of Engineering, Vukovarska 58, 51000 Rijeka, Croatia; leonarda.dosen@gmail.com (L.D.); janpelha@gmail.com (J.P.); goran.gregov@uniri.hr (G.G.)
* Correspondence: ekamenar@uniri.hr

Abstract

Soft robots are particularly suitable for in-pipe inspection, where locomotion must be achieved within confined, curved, and geometrically constrained environments without damaging the pipe wall. In this context, structural compliance is not only a safety feature but also a functional design principle, enabling the robot to adapt to the pipe geometry, maintain distributed contact, and generate locomotion through controlled anchoring and extension–contraction cycles. This study presents the design, fabrication, and experimental validation of an earthworm-inspired soft pneumatic robot for in-pipe inspection. The robot uses inflatable anchoring elements for alternating radial anchoring and pneumatic bellows actuators for extension–contraction cycles, enabling locomotion while maintaining stable contact with the pipe wall. A laboratory-scale prototype was fabricated using additive manufacturing and evaluated with a dedicated pneumatic and control system. Experiments were conducted to determine locomotion performance, operating pressures, actuation timing, friction characteristics, bend negotiation, and load capacity. The optimal anchoring pressure was only 0.1 bar, demonstrating that reliable contact with the pipe wall can be achieved at a very low pneumatic pressure. The robot achieved average locomotion speeds of 21.07 mm/s in horizontal and 20.59 mm/s in vertical PVC pipes, successfully traversed a 90° pipe bend, and demonstrated a maximum vertical load capacity of 1.2 kg. These results demonstrate the feasibility of the proposed biomimetic soft robotic concept for in-pipe inspection and provide a basis for future development toward autonomous operation and industrially relevant testing.

Keywords: soft robotics; in-pipe inspection; biomimetic robot; pneumatic actuator; earthworm-inspired locomotion; additive manufacturing

Check for updates

Academic Editors: Yanhong Peng, Fangchao Hu and Yi Li

Received: 16 July 2026
Revised: 7 August 2026
Accepted: 8 August 2026
Published: 11 August 2026

Copyright: © 2026 by the authors. Licensee MDPI, Basel, Switzerland. This article is an open access article distributed under the terms and conditions of the Creative Commons Attribution (CC BY) license.

1. Introduction

The safe and reliable operation of pipeline networks is essential for the continuous transportation of oil and gas. During long-term operation, pipelines are exposed to mechanical, chemical, and environmental degradation mechanisms that may lead to corrosion, material defects, leakage, deposits, or flow restrictions. Regular in-pipe inspection therefore plays an important role in preventive maintenance, condition assessment, and safe operation of pipeline infrastructure [1,2].

Pipeline inspection is a demanding application for mobile robots because the robot must operate inside a confined space while maintaining reliable contact with the pipe wall. Locomotion becomes particularly challenging in bends, elbows, regions with local diameter variations, contaminated surfaces, limited-access areas, and vertical pipe sections,

where the robot must maintain traction, avoid jamming, and support its own weight. Conventional in-pipe robots, such as wheeled, tracked, screw-driven, or wall-pressed mechanisms, can provide effective propulsion in many cases, but their performance often depends on sufficient traction, accurate alignment, and mechanical adaptation to the pipe geometry [3,4]. These requirements become especially challenging in narrow or curved pipelines, where rigid mechanisms may slip, jam, or require complex steering and diameter-adaptation systems [5].

Soft pneumatic actuation is well suited for in-pipe locomotion because compliant elements can adapt to confined and curved pipe geometries while maintaining distributed contact with the pipe wall. Although soft robots may incorporate rigid structural components to provide mechanical support, guidance, and integration of the pneumatic system, their primary locomotion capabilities are achieved through compliant pneumatic elements. These elements can reduce the risk of jamming and generate anchoring and extension–contraction-based motion [6,7]. Beyond conventional pneumatic architectures, recent bioinspired soft-robotic research has also explored multifunctional tubular actuators capable of reproducing flagellar and ciliary motion [8], as well as hydrogel-based artificial muscles integrating sensing and actuation [9]. Biomimetic locomotion is especially relevant in this context, since organisms such as snakes, caterpillars, and earthworms move effectively through constrained environments by coordinating body deformation with contact forces from the surrounding surface [10–12]. Among these biological examples, earthworm locomotion is particularly suitable for in-pipe robots because it relies on alternating radial anchoring and axial body motion [13,14]. Recent worm- and earthworm-inspired in-pipe robots have adopted this principle by combining radial anchoring with axial extension–contraction to generate motion in confined pipe environments [15–17]. Hybrid soft–rigid worm-like designs have also been proposed to combine the adaptability of soft anchoring elements with the traction and structural support of rigid mechanisms [18–20]. Table 1 compares representative experimentally validated biomimetic pneumatic robots developed for in-pipe inspection, including the prototype proposed in this work.

Beyond mechanical design, modeling and control remain important challenges for soft robotic systems because their behavior is strongly nonlinear, compliant, and affected by contact with the environment [6,7]. Koopman-based and data-driven approaches have been explored for modeling and control of nonlinear soft robotic systems [21]. Although the present work focuses on prototype development and experimental characterization, such approaches represent a relevant direction for future autonomous operation of soft in-pipe robots.

The motivation for this work arises from the need for a compact robotic platform capable of moving through constrained pipe sections while maintaining stable contact with the pipe wall. In collaboration with INA d.d., the Croatian national oil and gas company headquartered in Zagreb, Croatia, design requirements were derived from the operational characteristics of a liquefied petroleum gas (LPG) transmission pipeline. These requirements motivated the development of a biomimetic soft pneumatic robot inspired by earthworm locomotion. Soft pneumatic actuation offers a promising alternative for such applications, but experimentally validated soft robotic solutions for reliable in-pipe locomotion remain relatively limited, particularly with respect to anchoring pressure, actuation timing, friction behavior, bend traversal, vertical locomotion, and load capacity. Therefore, this study investigates the feasibility of the proposed biomimetic locomotion strategy by designing, fabricating, and experimentally validating a soft pneumatic robot for in-pipe inspection under controlled laboratory conditions.

Table 1. Comparison of representative biomimetic soft robots for in-pipe inspection.

References	Bio-Inspiration	Actuation Mechanism	Control	Pressure Mode	Pipe ID (mm)	Vertical	90° Bend	Pressure (bar)	Payload	Speed (mm/s)
Lee et al. [11]	Snake	Vacuum modules	Open-loop cyclic	NP	NR	×	✓	−0.15	2.5× robot mass	NR
Sheng et al. [12]	Caterpillar	Bellows + friction feet	Closed-loop pressure	PP	NR	×	✓	0.01–0.50	NR	1.32 (C)
Zhao et al. [15]	Earthworm	EPA + REPA anchors	Sequential open-loop	PP	90	✓	✓	NR	NR	1.27 (H); 0.39 (V)
Li et al. [16]	Inchworm	Expansion anchors + telescopic actuator	Sequential open-loop	PP	90–110	✓	✓	NR	NR	NR
Rezaei et al. [17]	Earthworm	Axial actuator + grippers	Sequential open-loop	PP	54	NR	NR	0–0.75	NR	≈9
Fang et al. [18]	Earthworm	Soft anchors + motorized telescopic body	Sequential open-loop	PP	NR	✓	✓	NR	NR	9.5–12.7
Zhang et al. [19]	Inchworm	Parallel ePSAs + flexible feet	Open-loop gait	PP	55–75	✓	✓	0–1	NR	20.1 (H); 12.9 (V)
Lin et al. [20]	NR	Single PAM + buckling ribbons	Open-loop on/off	PP	51–56	✓	✓ [a]	0.9–1.2	NR	NR
This work	Earthworm	Bellows + balloon anchors	Open-loop state machine	PP + NP	71.2	✓	✓	0.1; −0.4 to 0.4	5× robot mass	21.07 (H); 20.59 (V)

PP = positive pressure; NP = negative pressure (vacuum); EPA = elongation pneumatic actuator; REPA = radial expansion pneumatic actuator; PAM = pneumatic artificial muscle; ePSA = extensible pneumatic soft actuator; NR = not reported; ID = Inner diameter; H = horizontal; V = vertical; C = curved pipe. For this work, pressure values indicate anchoring pressure and bellows actuation pressure, respectively. [a] Lin et al. [20] demonstrated traversal of a 90° sweep elbow and a 45° elbow, but not the tighter 90° elbow evaluated in their study.

To address these challenges, this work presents the development and experimental validation of a biomimetic soft pneumatic robot for in-pipe inspection inspired by earthworm locomotion. The robot combines two modular, low-pressure inflatable anchoring elements with two serially connected pneumatic bellows actuators, building on actuator concepts investigated in our previous research [22,23]. Each anchoring element incorporates an inflatable balloon supplied through internal pneumatic passages, thereby enabling compliant contact with the pipe wall without external tubing around the anchor. The serially connected bellows provide the axial stroke required for locomotion while maintaining sufficient flexibility to negotiate curved pipe sections. The main distinction of the proposed platform lies in the combination of low-pressure pneumatic anchoring, serial bellows actuation, and systematic experimental characterization of the complete locomotion cycle within a single laboratory-scale platform. As summarized in Table 1, the study evaluates not only locomotion speed but also anchoring pressure, frictional pipe-wall interaction, inflation and deflation timing, bellows stroke, vertical locomotion, load capacity, and traversal of a 90° pipe bend.

The main contributions of this work are summarized as follows:

- Development of a modular biomimetic in-pipe robot that combines two low-pressure inflatable anchoring elements with integrated internal pneumatic passages and two serially connected bellows actuators, enabling both axial locomotion and traversal of curved pipe sections;
- Experimental characterization of the low-pressure anchoring mechanism, demonstrating reliable pipe-wall engagement at an anchoring pressure of 0.1 bar, with an average effective friction coefficient of approximately 2;

- Identification of the principal operating parameters governing the locomotion cycle, including anchoring pressure, vacuum-assisted deflation, actuation timing, and bellows stroke;
- Demonstration of comparable locomotion performance in horizontal and vertical pipes, with average speeds of 21.07 mm/s and 20.59 mm/s, respectively;
- Experimental demonstration of vertical transport of a 1.2 kg load, corresponding to approximately five times the robot's own mass, and successful traversal of a 90° pipe bend;
- Identification of practical limitations affecting future scale-up and autonomous operation, including pneumatic line length, tether resistance, anchor geometry, payload integration, and onboard pneumatic supply.

The remainder of this paper is organized as follows. Section 2 presents the design requirements, locomotion concept, mechanical design and fabrication of the proposed biomimetic soft pneumatic robot, together with the experimental setup and control system. Section 3 presents the experimental evaluation of the robot, including its anchoring and locomotion performance. Finally, Section 4 summarizes the main conclusions and outlines directions for future research.

2. Materials and Methods

This section presents the development of the biomimetic soft pneumatic robot for in-pipe inspection. First, the reference application and design requirements are defined based on the target pipeline geometry. The biomimetic locomotion concept is then introduced, followed by the mechanical design, fabrication, assembly, and control system of the laboratory-scale prototype.

2.1. Reference Application and Design Requirements

The proposed robot was developed as a compact inspection platform for constrained pipe environments, with the capability to carry lightweight inspection sensors, such as a forward-facing camera for visual inspection of the internal pipe surface. The functional and dimensional requirements were defined using an LPG transmission pipeline operated by INA d.d. as the reference application. The considered pipeline section connects Ivanić-Grad and Zagreb, Croatia, and has an inner diameter of 85.6 mm, which defines the available installation space for the robot. In addition, the capability to negotiate 90° pipe bends was identified as a key design requirement.

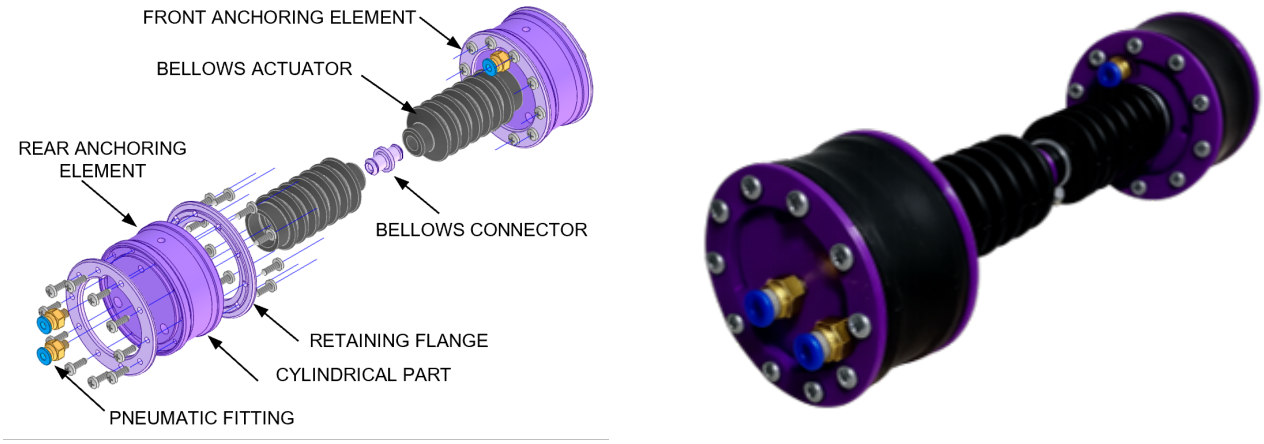
Since the primary objective of this study was to evaluate the feasibility and performance of the proposed locomotion concept rather than to develop a full-scale industrial inspection system, a laboratory-scale prototype was adopted. Accordingly, the experimental evaluation was performed in a commercially available DN75 polyvinyl chloride (PVC) pipe, whose internal dimensions closely match those of the reference pipeline. To evaluate the robot's ability to move through curved pipeline sections, a laboratory-scale 90° pipe elbow was designed and fabricated via additive manufacturing, as a steel elbow with the required dimensions was not commercially available. The elbow geometry was defined according to the DIN 2605 T2 standard and scaled to match the dimensions of the experimental DN75 PVC pipeline. This approach enabled controlled experimental validation of the proposed locomotion strategy while preserving the principal geometric constraints of the target application.

2.2. Locomotion Concept, Mechanical Design and Fabrication

The proposed robot employs an earthworm-inspired locomotion mechanism based on alternating anchoring and axial body deformation. It consists of two pneumatically

actuated anchoring elements connected by two soft pneumatic bellows actuators arranged in series, as shown in Figure 1. Each anchoring element incorporates an inflatable elastic balloon that expands radially under positive pressure to establish frictional contact with the pipe wall. Locomotion is generated through cyclic extension and contraction of the bellows actuators under positive and negative pressure, respectively, producing the axial displacement of the robot. Locomotion is achieved through alternating rear and front anchoring synchronized with the extension–contraction cycle of the bellows actuators.

The prototype was developed through an iterative design process in which the design was progressively refined based on experimental observations. Each anchoring element consists of a cylindrical part and two retaining flanges secured by screws, which clamp an elastic rubber balloon and provide both mechanical fixation and pneumatic sealing (Figure 1a). The initial design of the anchoring elements was oversized, resulting in insufficient radial clearance to allow proper expansion and sealing of the inflatable balloon. Furthermore, air leakage occurred between the inflatable balloon and the flanges. These limitations were eliminated by reducing the overall dimensions of the anchoring element and introducing interlocking grooves between the anchoring cylindrical part and the retaining flanges. The modified geometry significantly improved balloon sealing while providing sufficient clearance for smooth locomotion inside the pipe.



(**a**) (**b**)

Figure 1. Development of the proposed biomimetic soft robot: (**a**) exploded CAD view illustrating the main robot components; (**b**) assembled laboratory prototype.

Experimental evaluation further demonstrated that replacing a single bellows actuator with two actuators connected in series increased the available stroke and improved the robot's capability to traverse curved pipe sections, resulting in enhanced locomotion performance. Consequently, the final prototype employs two commercially available Una Scorpion Z-1023 rubber bellows (Una Scorpion d.o.o., Inđija, Serbia) connected in series as the pneumatic actuators.

The robot components were designed using Autodesk Inventor Professional 2026 (Autodesk Inc., San Francisco, CA, USA) and manufactured using fused filament fabrication (FFF) additive manufacturing. The anchoring cylindrical part, retaining flanges, and bellows connector were fabricated using a Flashforge Creator 3 Industrial 3D printer (Flashforge, Jinhua, China) with eSUN PLA+ filament (Shenzhen eSUN Industrial Co., Ltd., Shenzhen, China). PLA+ was selected because of its high dimensional accuracy, sufficient mechanical strength, and ease of fabrication, making it suitable for rapid prototyping of functional robotic components. The printed parts were manufactured using a nozzle temperature of 220 °C, a build platform temperature of 55 °C, a layer height of 0.1 mm, and

an infill density of 30% with a cubic infill pattern. These printing parameters provided adequate dimensional accuracy for the assembly interfaces while maintaining sufficient structural rigidity and minimizing the overall weight of the robot.

The compressed air supply to the anchoring elements and pneumatic bellows actuators was enabled by design of anchoring elements with internal air passages and M5 pneumatic fittings (Pneuflex Pneumatic Co., Ltd., Cixi, Ningbo, China) connected to PUN-4 × 0.75 polyurethane pneumatic tubing (Festo SE & Co. KG, Esslingen am Neckar, Germany). The pneumatic fitting on the rear anchoring element distributes compressed air to the rear rubber balloon and the central bellows actuators. A cylindrical passage is also provided through the rear anchoring element, through which a pneumatic tube is routed to the pneumatic fitting on the front anchoring element, which then supplies the front balloon. Following fabrication and assembly, the completed laboratory prototype (Figure 1b) had an overall length of 207 mm in the neutral state, a maximum outer diameter of 65 mm, and a total mass of 240 g.

2.3. Experimental Setup and Control System

The experiments were conducted at the Laboratory of Hydraulics and Pneumatics, University of Rijeka, Faculty of Engineering, using a CECCATO CSM 7.5 air compressor equipped with an air preparation unit (Ceccato S.p.A., Grisignano di Zocco, Italy), three FESTO VPPI-5L-3-G18-1V1H-V1-S1D proportional pressure regulators, and two FESTO VN-05-H-T2-PQ1-VQ1-RQ1 vacuum ejectors (Festo SE & Co. KG, Esslingen am Neckar, Germany). The vacuum ejectors operate according to the Venturi principle, whereby compressed air flowing through a converging nozzle generates negative pressure. For the selected ejectors, an inlet pressure of 5 bar provides a maximum negative pressure of approximately −0.9 bar.

Robot control and experimental data acquisition were implemented on an NI myRIO-1900 embedded controller (National Instruments Corporation, Austin, TX, USA) and programmed in the LabVIEW development environment. The control architecture was designed to provide independent pressure regulation of the rear anchoring element, the central bellows actuators, and the front anchoring element using three proportional pressure regulators operating over an input voltage range of 0–5 V, corresponding to an output pressure range of −1 to 1 bar. The desired pressure values were converted into analog control voltages using a linear voltage–pressure relationship and subsequently transmitted from the NI myRIO controller to the proportional pressure regulators, enabling independent pressure regulation of each pneumatic actuator.

The control software was implemented in LabVIEW as a cyclic state-based sequence corresponding to the earthworm-inspired locomotion pattern. Each locomotion cycle consists of six sequential actuation steps in which positive or negative pressure is applied to the rear anchoring element, bellows actuator, and front anchoring element according to predefined timing parameters. The duration of each step and the corresponding pressure levels can be adjusted independently through the graphical user interface, enabling straightforward optimization of the locomotion cycle. The graphical user interface also provides real-time monitoring and adjustment of the operating parameters, including the pressure values, the duration of each locomotion step, and the corresponding analog control voltages. In addition, the software provides functions for starting, stopping, pausing, and reversing the locomotion direction. Reverse locomotion is achieved by executing the actuation sequence in the opposite order while preserving the same control algorithm. The control software is available from the authors upon reasonable request.

Following prototype assembly and implementation of the control system, preliminary experiments were conducted to verify the functionality of the proposed robot before

quantitative performance evaluation. Initial tests confirmed stable locomotion in a PVC pipe, demonstrating the feasibility of the proposed six-step earthworm-inspired locomotion cycle as illustrated in Figure 2. Also, experimental validation demonstrated successful locomotion through the 90° pipe bend, confirming the suitability of the proposed biomimetic soft robotic concept for navigation in curved pipeline sections.

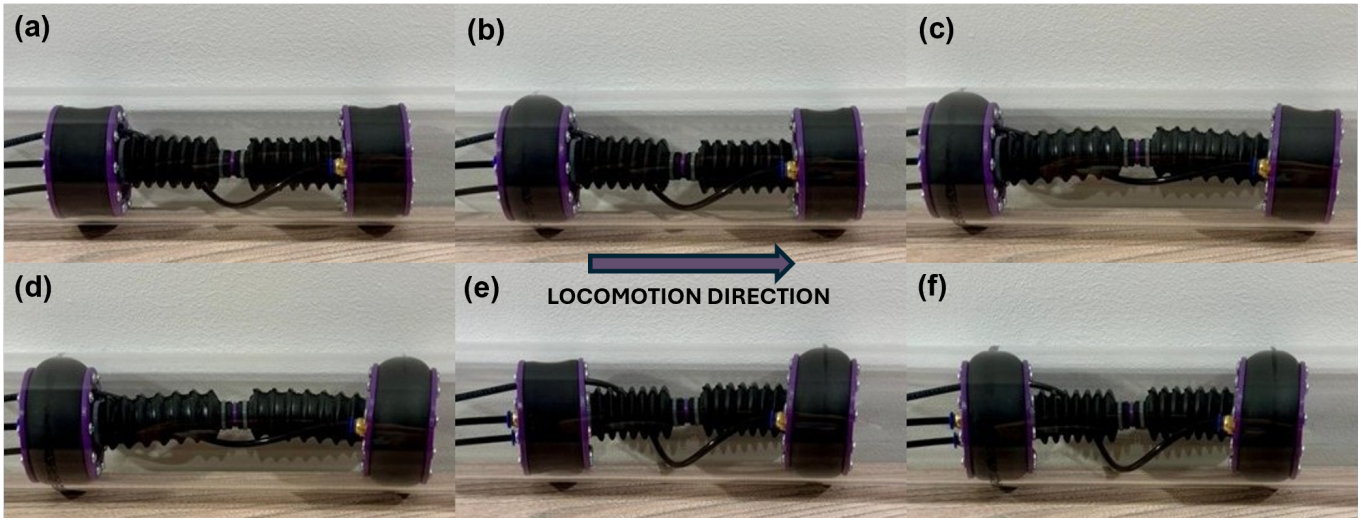


Figure 2. In-pipe locomotion cycle of the developed biomimetic soft pneumatic robot: (**a**) neutral state; (**b**) rear anchoring element inflates and fixes the rear part of the robot to the pipe wall; (**c**) bellows actuators extend and push the front element forward; (**d**) front anchoring element inflates and fixes the front element; (**e**) rear anchor is released and the bellows contract, pulling the rear element forward; and (**f**) rear anchoring element inflates again, preparing the robot for the next cycle.

3. Experimental Results and Discussion

This section presents the experimental results obtained under different operating conditions. The first set of experiments evaluated the anchoring performance by measuring the friction force between the robot's anchoring elements and the pipe wall, while the second assessed the locomotion performance under both unloaded and externally loaded conditions. Unless otherwise stated, each experiment was repeated five times, and the reported results correspond to the average values.

3.1. Experimental Evaluation of Anchoring Performance

The anchoring performance of the developed soft robot depends on the friction force generated between the inflated anchoring balloon and the inner pipe wall. Therefore, experiments were conducted to quantify the maximum friction force at different balloon pressures and to determine the optimal operating pressure for subsequent locomotion experiments. The selected pressure was required to provide sufficient anchoring force while avoiding excessive balloon deformation.

Since only the anchoring capability was investigated, the experiments were performed using a single anchoring element rather than the complete robot. The experimental setup consisted of an NI myRIO-1900 embedded controller, the previously described proportional pressure regulator, a Zemic H3G-C3-50kg-6B S-type load cell (Zemic Europe B.V., Etten-Leur, The Netherlands), and a custom measurement application developed in LabVIEW. The anchoring module was positioned inside a horizontal DN75 PVC pipe and connected to the load cell using a tensile rope. After inflating the balloon to the prescribed pressure, the anchoring module was pulled axially until anchoring failure occurred. The maximum extraction force was recorded as the friction force. Measurements were performed at balloon pressures of 0.025, 0.05, 0.075, and 0.1 bar. Figure 3a illustrates the relationship

between balloon pressure and the measured friction force, showing an approximately linear increase in friction force with increasing pressure, while the corresponding standard deviation values are provided in the Supplementary Materials (Table S1).

The nominal contact area between the inflated balloon and the pipe wall was approximated by the lateral surface area of the cylindrical anchoring element. Based on an anchoring element diameter of 65 mm and a contact width of 30 mm, the nominal contact area was calculated to be 6126 mm^2. For each applied pressure value, the normal force was estimated as the product of the applied pressure and the nominal contact area. This estimate was based on Pascal's law, according to which pressure in the enclosed fluid is transmitted throughout the balloon, together with the simplifying assumption that the internal pressure acts uniformly over the entire nominal contact region. The effective friction coefficient was subsequently calculated as the ratio of the measured friction force to the estimated normal force. However, although the internal balloon pressure can be considered approximately uniform, deformation and membrane tension result in a spatially non-uniform contact-pressure distribution between the balloon and the pipe wall, while the actual contact area varies with inflation. Therefore, the calculated coefficient represents an effective system-level value rather than an intrinsic Coulomb friction coefficient of the rubber balloon–PVC material pair. The experimental and calculated results are summarized in Table 2, yielding an average effective friction coefficient of approximately 2. This value is specific to the tested anchoring geometry, pressure range, and pipe material. Since the actual contact area and contact-pressure distribution were not measured, the uncertainty associated with this approximation could not be quantified directly. The maximum friction force of 126.1 N was achieved at a balloon pressure of 0.1 bar without observable balloon deformation, and this pressure was therefore selected as the operating pressure for all subsequent locomotion experiments.

Table 2. Maximum friction force, normal force, and coefficient of friction at different balloon pressures.

Pressure, Bar	Friction Force, N	Normal Force, N	Effective Friction Coeff., -
0.025	26.66	15.31	1.74
0.05	56.66	30.63	1.85
0.075	103.44	45.94	2.25
0.1	126.07	61.26	2.06

Following the selection of the operating balloon pressure, the dynamic response of the anchoring elements was experimentally evaluated to determine the minimum inflation and deflation times required to establish and release reliable anchoring during the locomotion cycle. During these experiments, the anchoring element was subjected to an axial pulling force, while the resulting friction force was continuously measured using a load cell. The actuation time was measured from the instant at which the LabVIEW control system sent the command signal to the proportional pressure regulator to the instant at which the anchoring element stopped moving during balloon inflation or began to slip during balloon deflation. As previously stated, the proportional pressure regulators operate over an input voltage range of 0–5 V, corresponding to an output pressure range of −1 to 1 bar. Each actuation step must be sufficiently long to allow the corresponding pneumatic element to reach its target state before the subsequent step is initiated. Insufficient actuation time results in incomplete anchoring, thereby reducing the overall locomotion performance. This procedure therefore accounts for the overall system response between command activation and the mechanical establishment or release of anchoring.

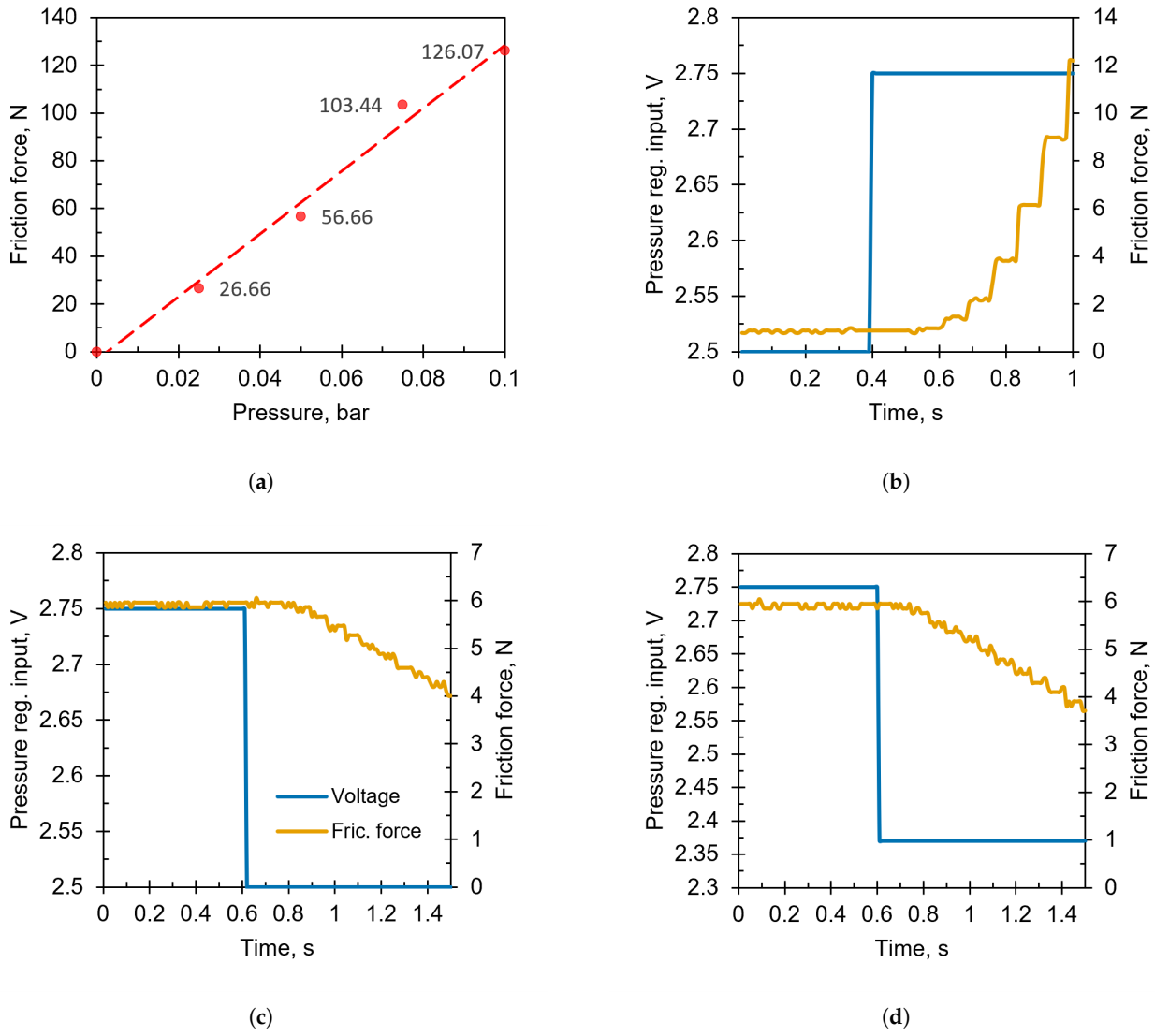


Figure 3. Experimental results of anchoring performance: (**a**) friction force over pressure; (**b**) time histories of pressure regulator input voltage and friction force during balloon inflation; (**c**) time histories of pressure regulator input voltage and friction force during passive balloon deflation; and (**d**) time histories of pressure regulator input voltage and friction force during active balloon deflation.

The inflation response of the anchoring balloon was first investigated using a single anchoring element positioned inside a horizontal PVC pipe and subjected to an axial pulling force. At $t = 0.4$ s, a step voltage signal of 2.75 V was applied to the proportional pressure regulator, corresponding to a target pressure setpoint of 0.1 bar. This setpoint represents the maximum target pressure rather than the instantaneous pressure inside the balloon. Reliable anchoring was established at a substantially lower balloon pressure of approximately 0.01 bar; therefore, the target pressure of 0.1 bar was not reached during this test. As shown in Figure 3b, the minimum friction-force threshold of approximately 4 N required for reliable anchoring and prevention of further axial motion was reached at $t = 0.78$ s, corresponding to a minimum inflation time of 0.38 s.

The deflation response was subsequently evaluated using the same anchoring element positioned inside a vertical PVC pipe. Two operating conditions were investigated: passive deflation by venting the balloon to atmospheric pressure and active deflation by applying a step voltage signal of 2.375 V to the proportional pressure regulator, corresponding to a target negative pressure setpoint of −0.05 bar. The deflation time was defined as the interval between activation of the deflation command and the onset of sliding of the anchoring element due to insufficient friction against the pipe wall. Passive deflation (Figure 3c) required 0.45 s, whereas active deflation assisted by negative pressure (Figure 3d) reduced this time to 0.36 s. Because the shorter deflation time directly reduces the duration of the locomotion cycle, active deflation was adopted in all subsequent experiments. Detailed standard deviation values for the inflation and deflation times are provided in the Supplementary Materials (Table S2).

It should be noted that all previously reported actuation times were obtained for the unloaded robot. For each load-carrying experiment, the actuation times were determined following the same measurement procedure. In all cases, the pneumatic system was connected using pneumatic pipes with a length of approximately 2 m. The pneumatic pipe length directly influences the inflation and deflation dynamics of the pneumatic actuators, as longer pneumatic pipes increase both the internal air volume and the flow resistance. Consequently, the longer pneumatic supply pipes required for practical pipeline inspection are expected to increase the duration of each locomotion step and reduce the overall locomotion speed. This limitation should be taken into consideration in the future development of the proposed semi-automated control system for industrial-scale applications.

3.2. Experimental Evaluation of Locomotion Performance

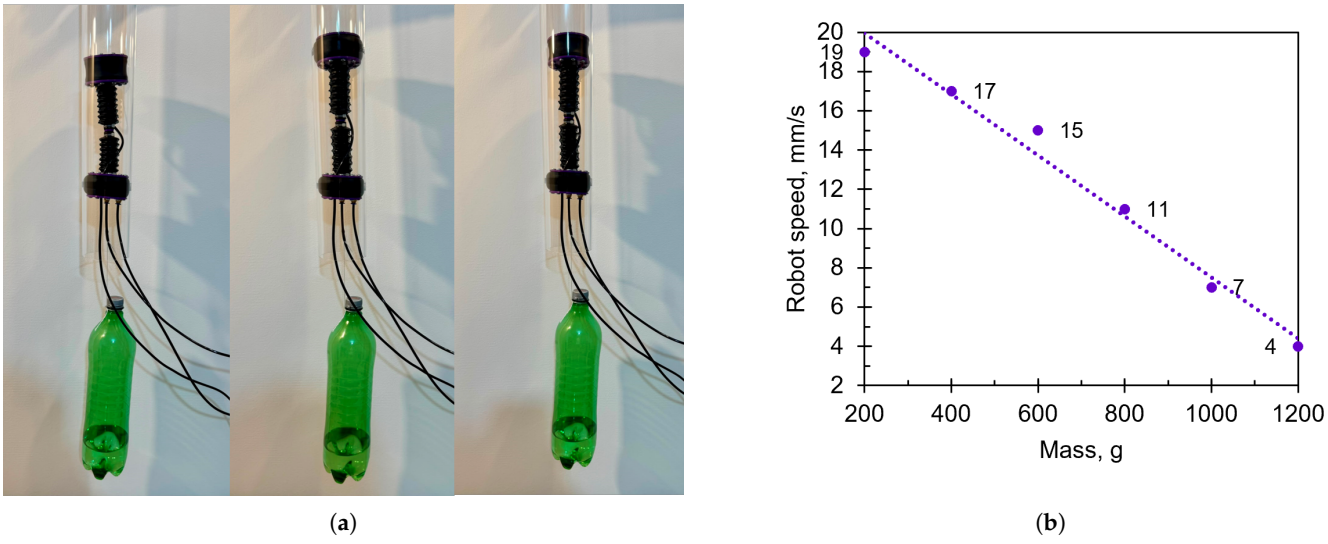
The locomotion performance of the proposed robot was evaluated using the operating parameters determined in the previous experiments for the anchoring elements. The bellows actuators were operated at a positive pressure of 0.4 bar and a negative pressure of −0.4 bar, corresponding to the maximum pressures that could be repeatedly applied without structural damage or excessive deformation. The actuation dynamics were determined from high-speed video analysis, yielding expansion and contraction times of 0.7 s and 0.8 s, respectively. Under these operating conditions, the bellows actuators provided a stroke of 70 mm, which was adopted for all subsequent locomotion experiments.

The average locomotion speed was first evaluated under unloaded conditions. The robot traversed an effective distance of 1770 mm in a horizontal DN75 PVC pipe at an average speed of 21.07 mm/s. The same experiment was subsequently performed in a vertical pipe orientation, resulting in an average speed of 20.59 mm/s. The difference between the two configurations was less than 3%, demonstrating that the anchoring elements provide sufficient friction to support the robot's weight while maintaining stable locomotion independently of pipe orientation.

Additional experiments were conducted using lower bellows actuator pressures of ±0.2 bar. Under these conditions, the bellows actuator stroke decreased from 70 mm to 40 mm, reducing the average locomotion speed to approximately 11.9 mm/s. These results indicate that the locomotion speed is primarily governed by the stroke of the bellows actuators achieved during each actuation cycle. It should be emphasized that all experiments were conducted with approximately 2 m of pneumatic tubing connected to the robot, which introduced additional resistance during locomotion. Consequently, the reported performance reflects the behavior of the current laboratory-scale prototype under these experimental conditions.

The load-carrying capability of the proposed robot was subsequently evaluated in a vertical pipeline by attaching external masses to the rear anchoring module, as shown in Figure 4a. The experiments were conducted using payload masses ranging from 200 to 1200 g in increments of 200 g. As the payload increased, the average locomotion speed decreased progressively owing to the reduction in the effective bellows stroke (Figure 4b). The robot successfully transported payloads of up to 1.2 kg, corresponding to approximately five times its own mass, while maintaining reliable locomotion, although its speed decreased to 4 mm/s. No slippage of the anchoring elements was observed; instead, the payload capacity was limited by the approximately 13 N axial force generated by the bellows actuators at an operating pressure of 0.4 bar. Although higher payload capacities could be achieved using larger-diameter actuators rated for higher operating pressures, the resulting increase in actuator dimensions may affect the robot's ability to traverse 90° pipe bends and therefore requires further investigation. Detailed standard deviation values for the robot's locomotion speed under unloaded and loaded conditions are provided in the Supplementary Materials (Table S3).

To demonstrate the feasibility of integrating visual inspection capability into the developed robot, a lightweight BETAFPV C03 micro first-person-view (FPV) camera (Shenzhen Baida Moxing Co., Ltd., Shenzhen, China) was mounted on the front anchoring element and oriented in the direction of locomotion. The camera was selected for its compact dimensions, low mass, and wide field of view, which enable visual inspection of the internal pipe surface with minimal impact on the robot's locomotion. The power supply and video transmission cables were routed through dedicated passages integrated into the anchoring elements. Figure 5 shows the robot during in-pipe locomotion, together with representative images from the front-mounted camera. A video demonstrating the robot locomotion and the real-time in-pipe inspection view is provided as Video S1 in the Supplementary Material.



(**a**) (**b**)

Figure 4. Experimental evaluation of load-carrying performance: (**a**) vertical payload test setup showing the load carried by the developed robot and (**b**) robot speed as a function of payload.

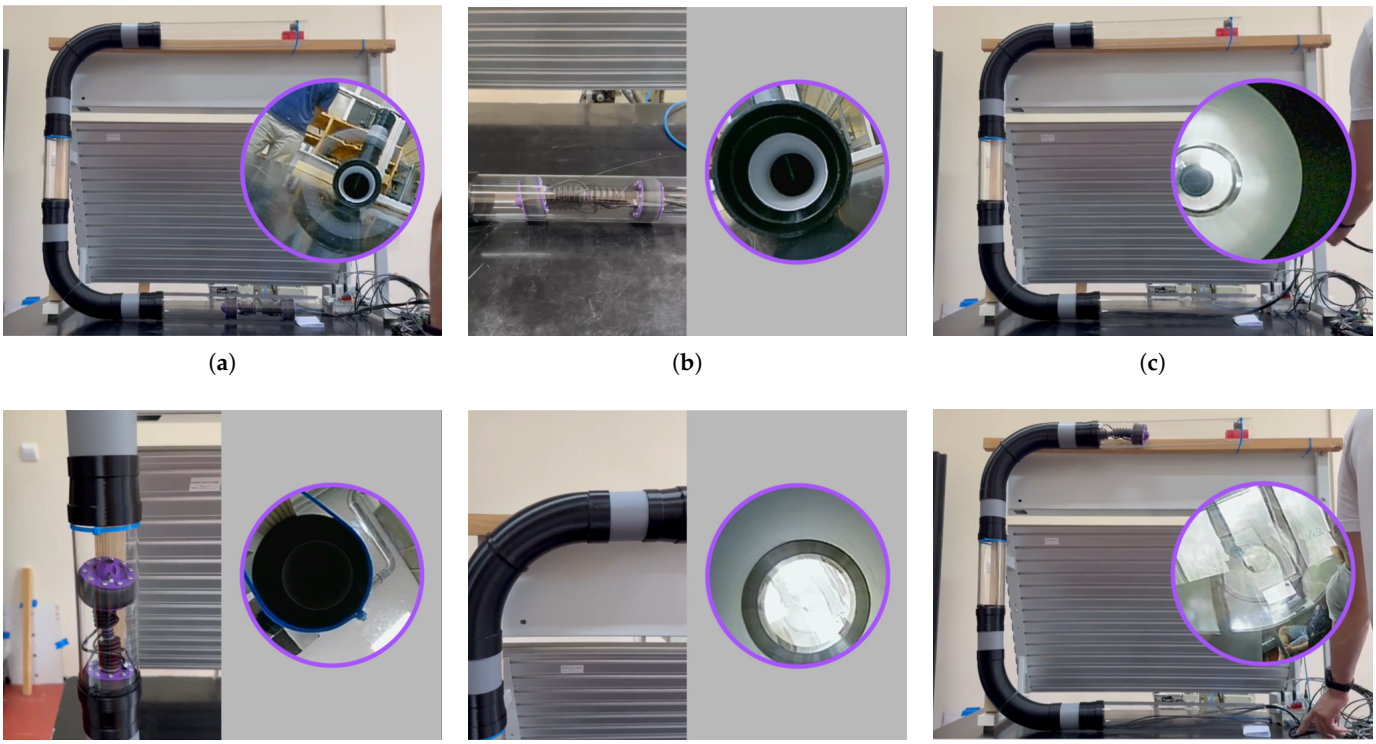


Figure 5. In-pipe robot locomotion and front-mounted camera-based inspection: (**a**) horizontal locomotion through the lower pipe section with the corresponding camera view of the pipe interior; (**b**) close-up of the robot moving inside the transparent pipe section and the corresponding forward-facing camera image; (**c**) transition through the pipe bend with the camera view showing the internal pipe wall; (**d**) vertical locomotion inside the pipe and the corresponding camera image; (**e**) locomotion through the curved pipe section with the camera view of the bend region; and (**f**) completed traversal through the pipe loop with the corresponding inspection image.

4. Conclusions

This paper presented the design, fabrication, and experimental validation of a biomimetic soft pneumatic robot for in-pipe inspection inspired by earthworm locomotion. The proposed robot employs alternating anchoring and extension–contraction cycles generated by inflatable anchoring elements with balloons and a pair of pneumatic bellows actuators, providing compliant locomotion suitable for confined pipeline environments.

Experimental investigations determined the optimal operating parameters of the pneumatic system. For the anchoring elements, an operating pressure of 0.1 bar provided the maximum friction force of 126 N without observable balloon deformation, corresponding to an average effective friction coefficient of approximately 2. The measured actuation times were 0.38 s for balloon inflation and 0.36 s for active balloon deflation using negative pressure. At an operating pressure of 0.4 bar, the measured expansion and contraction times of the bellows actuators were 0.7 s and 0.8 s, respectively, with a corresponding stroke of 70 mm. The developed soft robot prototype achieved average locomotion speeds of 21.07 mm/s and 20.59 mm/s in horizontal and vertical pipelines, respectively, demonstrating reliable locomotion independent of pipe orientation. Furthermore, the robot successfully traversed a 90° pipe bend and transported payloads of up to 1.2 kg in the vertical configuration, confirming the effectiveness of the proposed biomimetic locomotion strategy.

Although these results validate the feasibility of the proposed concept, several limitations associated with the laboratory-scale prototype were identified. In particular, the length of the pneumatic supply pipes significantly influences actuator response time and

overall locomotion speed, representing an important challenge for large-scale pipeline deployment. In addition, because the anchoring experiments were performed in PVC pipes, the calculated effective friction coefficient should not be directly generalized to steel, corroded, wet, or contaminated industrial pipelines. Therefore, further experimental evaluation is required to assess the robot's behavior under the most adverse operating conditions representative of real industrial pipelines.

Future work will therefore focus on evaluating the anchoring behavior on pipe materials and surface conditions representative of real gas pipelines, improving the anchoring mechanism through optimized geometry and higher-friction materials, increasing system autonomy by integrating a compact onboard pneumatic supply, implementing closed-loop pressure control, and incorporating advanced inspection sensors to enhance the robot's capability for practical in-pipe inspection.

Supplementary Materials: The following supporting information can be downloaded at: https://www.mdpi.com/article/10.3390/act15080435/s1.

Author Contributions: Conceptualization, L.D., J.P., G.G. and E.K.; methodology, L.D., J.P., G.G. and E.K.; validation, L.D. and J.P.; formal analysis, L.D. and J.P.; investigation, L.D. and J.P.; resources, G.G. and E.K.; data curation, L.D. and J.P.; writing—original draft preparation, L.D., J.P., G.G. and E.K.; writing—review and editing, G.G. and E.K.; visualization, L.D. and J.P.; supervision, G.G. and E.K.; project administration, G.G. and E.K. All authors have read and agreed to the published version of the manuscript.

Funding: This work has been supported by the Croatian Science Foundation under grant UIP-2025-02-1541 and by the University of Rijeka under grant uniri-iz-25-231.

Institutional Review Board Statement: Not applicable.

Informed Consent Statement: Not applicable.

Data Availability Statement: The data supporting the findings of this study are available from the corresponding author upon reasonable request.

Acknowledgments: The authors gratefully acknowledge INA d.d. (Zagreb, Croatia) for providing materials and technical information used to define the reference pipeline application considered in this study.

Conflicts of Interest: The authors declare no conflicts of interest.

Abbreviations

The following abbreviations are used in this manuscript:

PVC	Polyvinyl chloride
FFF	Fused filament fabrication
FPV	First-person view
LPG	Liquefied petroleum gas

References

1. Zhang, J.; Sun, M.; Qin, L.; Lin, D.; Liu, C.; Li, J.; Li, C.; Wen, S.; Han, C. In-line inspection methods and tools for oil and gas pipeline: A review. *Int. J. Press. Vessel. Pip.* **2025**, *214*, 105409. [CrossRef]
2. Li, R. Current progress and prospects of in-line inspection techniques and data analysis methods for oil and gas pipelines. *You-Qi Chuyun* **2024**, *43*, 241–256. [CrossRef]
3. Verma, A.; Kaiwart, A.; Dubey, N.D.; Naseer, F.; Pradhan, S. A review on various types of in-pipe inspection robot. *Mater. Today Proc.* **2022**, *50*, 1425–1434. [CrossRef]
4. Ismail, I.N.; Anuar, A.; Sahari, K.S.M.; Baharuddin, M.Z.; Fairuz, M.; Jalal, A.; Saad, J.M. Development of in-pipe inspection robot: A review. In *Proceedings of the 2012 IEEE Conference on Sustainable Utilization and Development in Engineering and Technology (STUDENT), Kuala Lumpur, Malaysia, 6–9 October 2012*; IEEE: Piscataway, NJ, USA, 2013; pp. 310–315. [CrossRef]

5. Ma, Q.; Liang, W.; Zhou, P. A review on pipeline in-line inspection technologies. *Sensors* **2025**, *25*, 4873. [CrossRef] [PubMed]
6. Rus, D.; Tolley, M.T. Design, fabrication and control of soft robots. *Nature* **2015**, *521*, 467–475. [CrossRef] [PubMed]
7. Kim, S.; Laschi, C.; Trimmer, B. Soft robotics: A bioinspired evolution in robotics. *Trends Biotechnol.* **2013**, *31*, 287–294. [CrossRef] [PubMed]
8. Miao, J.; Zhang, T.; Li, G.; Guo, D.; Sun, S.; Tan, R.; Shi, J.; Shen, Y. Flagellar/ciliary intrinsic driven mechanism inspired all-in-one tubular robotic actuator. *Engineering* **2023**, *23*, 170–180. [CrossRef]
9. Zhou, Y.; Zhao, Y.; Zhao, D.; Guan, X.; Zhang, K.; Pi, Y.; Zhong, J. Sensing-actuating integrated asymmetric multilayer hydrogel muscle for soft robotics. *Microsyst. Nanoeng.* **2025**, *11*, 40. [CrossRef] [PubMed]
10. Pan, M.; Liu, M.; Lei, J.; Wang, Y.; Linghu, C.; Bowen, C.; Hsia, K.J. Bioinspired mechanisms and actuation of soft robotic crawlers. *Adv. Sci.* **2025**, *12*, 2416764. [CrossRef] [PubMed]
11. Lee, S.; Her, I.; Jung, W.; Hwang, Y. Snakeskin-Inspired 3D Printable Soft Robot Composed of Multi-Modular Vacuum-Powered Actuators. *Actuators* **2023**, *12*, 62. [CrossRef]
12. Sheng, X.; Xu, H.; Zhang, N.; Ding, N.; Zhu, X.; Gu, G. Multi-material 3D printing of caterpillar-inspired soft crawling robots with the pneumatically bellow-type body and anisotropic friction feet. *Sens. Actuators A Phys.* **2020**, *316*, 112398. [CrossRef]
13. Blewitt, G.; Cheneler, D.; Andrew, J.; Monk, S. A Review of Worm-Like Pipe Inspection Robots: Research, Trends and Challenges. *Soft Sci.* **2024**, *4*, 13. [CrossRef]
14. Chen, N.; Jiang, F.; Du, X.; Wu, Y.; Yan, L.; Zhang, R. Biomimetic Robots Inspired by Annelid Animals: Research Progress and Development Trend. *J. Bionic Eng.* **2025**, *22*, 2194–2235. [CrossRef]
15. Zhao, Y.; Huang, H.; Yuan, W.; Liu, X.; Cao, C. Worm-Inspired, Untethered, Soft Crawling Robots for Pipe Inspections. *Soft Robot.* **2024**, *11*, 639–649. [CrossRef] [PubMed]
16. Li, M.; Wang, G.; Wang, J.; Zheng, Y.; Jiao, X. Development of an Inchworm-Like Soft Pipe Robot for Detection. *Int. J. Mech. Sci.* **2023**, *253*, 108392. [CrossRef]
17. Rezaei, M.H.; Kolani, M.R.; Zareinejad, M. Earthworm-Inspired In-Pipe Soft Robot: Design, Modeling, and Implementation. In *Proceedings of the 2023 11th RSI International Conference on Robotics and Mechatronics, Tehran, Iran, 1 February 2023*; IEEE: Piscataway, NJ, USA, 2023; pp. 390–395. [CrossRef]
18. Fang, D.; Jia, G.; Wu, J.; Niu, X.; Li, P.; Wang, R.; Zhang, Y.; Zhang, J. A novel worm-like in-pipe robot with the rigid and soft structure. *J. Bionic Eng.* **2023**, *20*, 2559–2569. [CrossRef]
19. Zhang, Z.; Wang, X.; Wang, S.; Meng, D.; Liang, B. Design and modeling of a parallel-pipe-crawling pneumatic soft robot. *IEEE Access* **2019**, *7*, 134301–134317. [CrossRef]
20. Lin, Y.; Xu, Y.X.; Juang, J.Y. Single-actuator soft robot for in-pipe crawling. *Soft Robot.* **2023**, *10*, 174–186. [CrossRef] [PubMed]
21. Haggerty, D.A.; Banks, M.J.; Kamenar, E.; Cao, A.B.; Curtis, P.C.; Mezić, I.; Hawkes, E.W. Control of Soft Robots with Inertial Dynamics. *Sci. Robot.* **2023**, *8*, eadd6864. [CrossRef] [PubMed]
22. Gregov, G.; Ploh, T.; Kamenar, E. Design, Development and Experimental Assessment of a Cost-Effective Bellow Pneumatic Actuator. *Actuators* **2022**, *11*, 170. [CrossRef]
23. Gregov, G.; Vuković, T.; Gašparić, L.; Pongrac, M. Development, experimental assessment, and application of a Vacuum-Driven soft bending actuator. *Appl. Sci.* **2025**, *15*, 2557. [CrossRef]

Disclaimer/Publisher's Note: The statements, opinions and data contained in all publications are solely those of the individual author(s) and contributor(s) and not of MDPI and/or the editor(s). MDPI and/or the editor(s) disclaim responsibility for any injury to people or property resulting from any ideas, methods, instructions or products referred to in the content.